Cell Reports

IL-17 triggers the onset of cognitive and synaptic deficits in early stages of Alzheimer's disease

Graphical abstract

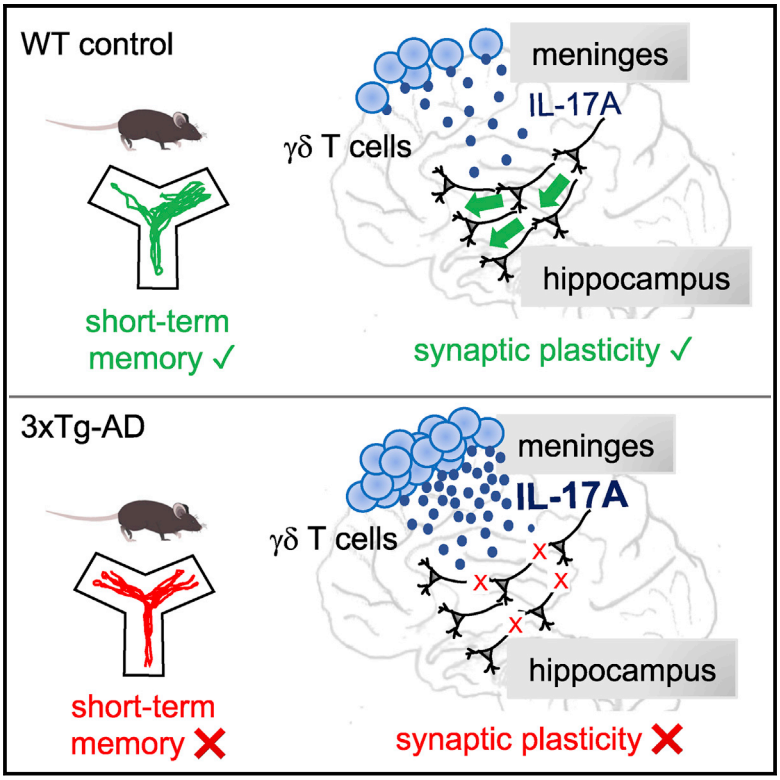

Highlights

- IL-17-producing cells accumulate in the brain and the meninges of 3xTg-AD mice
- The increase of IL-17 producers associates with short-term memory deficits
- Neutralization of IL-17 prevents cognitive impairments and synaptic dysfunction
- IL-17 triggers Alzheimer's disease onset independently of Aβ and tau pathology

Authors

Helena C. Brigas, Miguel Ribeiro, Joana E. Coelho, ..., Bruno Silva-Santos, Luísa V. Lopes, Julie C. Ribot

Correspondence

lvlopes@medicina.ulisboa.pt (L.V.L.), jribot@medicina.ulisboa.pt (J.C.R.)

In brief

Using a mouse model of Alzheimer's disease, Brigas et al. demonstrate that the onset of cognitive decline associates with an accumulation of IL-17-producing cells in the brain and the meninges. Targeting IL-17 into the ventricle prevents short-term memory and neuronal synaptic plasticity deficits at early stages of disease.

Brigas et al., 2021, Cell Reports *36*, 109574
August 31, 2021
https://doi.org/10.1016/j.celrep.2021.109574

Cell Reports

CellPress
OPEN ACCESS

Article

IL-17 triggers the onset of cognitive and synaptic deficits in early stages of Alzheimer's disease

Helena C. Brigas,[1] Miguel Ribeiro,[1] Joana E. Coelho,[1] Rui Gomes,[1,2] Victoria Gomez-Murcia,[3,4] Kevin Carvalho,[3,4] Emilie Faivre,[3,4] Sara Costa-Pereira,[1] Julie Darrigues,[1] Afonso Antunes de Almeida,[1] Luc Buée,[3,4] Jade Dunot,[5] Hélène Marie,[5] Paula A. Pousinha,[5] David Blum,[3,4] Bruno Silva-Santos,[1] Luísa V. Lopes,[1,6,*] and Julie C. Ribot[1,6,7,*]

[1]Instituto de Medicina Molecular João Lobo Antunes, Faculdade de Medicina, Universidade de Lisboa, Av. Professor Egas Moniz, 1649-028 Lisboa, Portugal

[2]Faculdade de Ciências de Lisboa, Universidade de Lisboa, 1749-016 Lisboa, Portugal

[3]Université Lille, Inserm, CHU Lille, U1172 - LilNCog - Lille Neuroscience & Cognition, 59000 Lille, France

[4]Alzheimer & Tauopathies, LabEx DISTALZ, Lille, France

[5]Université Côte d'Azur, CNRS, UMR 7275, Institute of Molecular and Cellular Pharmacology (IPMC), Valbonne, France

[6]These authors contributed equally

[7]Lead contact

*Correspondence: lvlopes@medicina.ulisboa.pt (L.V.L.), jribot@medicina.ulisboa.pt (J.C.R.)

https://doi.org/10.1016/j.celrep.2021.109574

SUMMARY

Neuroinflammation in patients with Alzheimer's disease (AD) and related mouse models has been recognized for decades, but the contribution of the recently described meningeal immune population to AD pathogenesis remains to be addressed. Here, using the 3xTg-AD model, we report an accumulation of interleukin-17 (IL-17)-producing cells, mostly γδ T cells, in the brain and the meninges of female, but not male, mice, concomitant with the onset of cognitive decline. Critically, IL-17 neutralization into the ventricles is sufficient to prevent short-term memory and synaptic plasticity deficits at early stages of disease. These effects precede blood-brain barrier disruption and amyloid-beta or tau pathology, implying an early involvement of IL-17 in AD pathology. When IL-17 is neutralized at later stages of disease, the onset of short-memory deficits and amyloidosis-related splenomegaly is delayed. Altogether, our data support the idea that cognition relies on a finely regulated balance of "inflammatory" cytokines derived from the meningeal immune system.

INTRODUCTION

Alzheimer's disease (AD) is a highly prevalent neurodegenerative disorder characterized by cognitive deficits due to synaptic dysfunction and sequential formation of amyloid-beta (Aβ) plaques and hyperphosphorylated tau tangles. There is currently no effective treatment for AD (Dubois et al., 2010; Reitz and Mayeux, 2014), urging the discovery of additional mechanisms underlying the etiology of the disease.

Neuroinflammation, characterized by increased proinflammatory cytokines, infiltrating immune cells, and activated glial cells, is increasingly recognized as a prominent player in AD. However, the role of the immune system is not limited to the brain parenchyma, as it comprises complex interactions between the central nervous system (CNS) and the peripheral systems (Louveau et al., 2015). For instance, T cells, B cells, dendritic cells, innate lymphoid cells, and natural killer (NK) cells reside in the healthy meninges—a direct interface between the brain parenchyma and the peripheral organs (Aspelund et al., 2015; Louveau et al., 2015; Gadani et al., 2017; Korin et al., 2017). Importantly, immune cells and their soluble mediators, namely cytokines, play a key role in CNS function by modulating neuronal connectivity and thus impacting on sensory function (Chen et al., 2017), social behavior (Filiano et al., 2016), as well as learning and memory (Derecki et al., 2010; Monteiro et al., 2016; Ribeiro et al., 2019). It was recently shown that, upon aging and in AD, meningeal lymphatic vasculature deteriorates, thus impairing cognition (Da Mesquita et al., 2018). Furthermore, the ablation of meningeal lymphatic vessels worsened the outcome of anti-Aβ immunotherapy in the 5xFAD mouse model (Da Mesquita et al., 2021). However, the role of specific meningeal immune populations and their molecular mediators in the context of AD was never addressed.

We have recently reported that γδ T cells are a major source of interleukin-17A (IL-17) in the healthy meninges, which promotes specifically short-term memory by supporting glutamatergic synaptic plasticity of CA1 hippocampal neurons (Ribeiro et al., 2019). Additionally, IL-17 produced by astrocytes after stroke was also shown to have a beneficial role by promoting tissue repair (Lin et al., 2016). In contrast, murine IL-17-producing cells have been linked to experimental autoimmune encephalomyelitis (EAE) (Sutton et al., 2009), cerebral ischemia-reperfusion

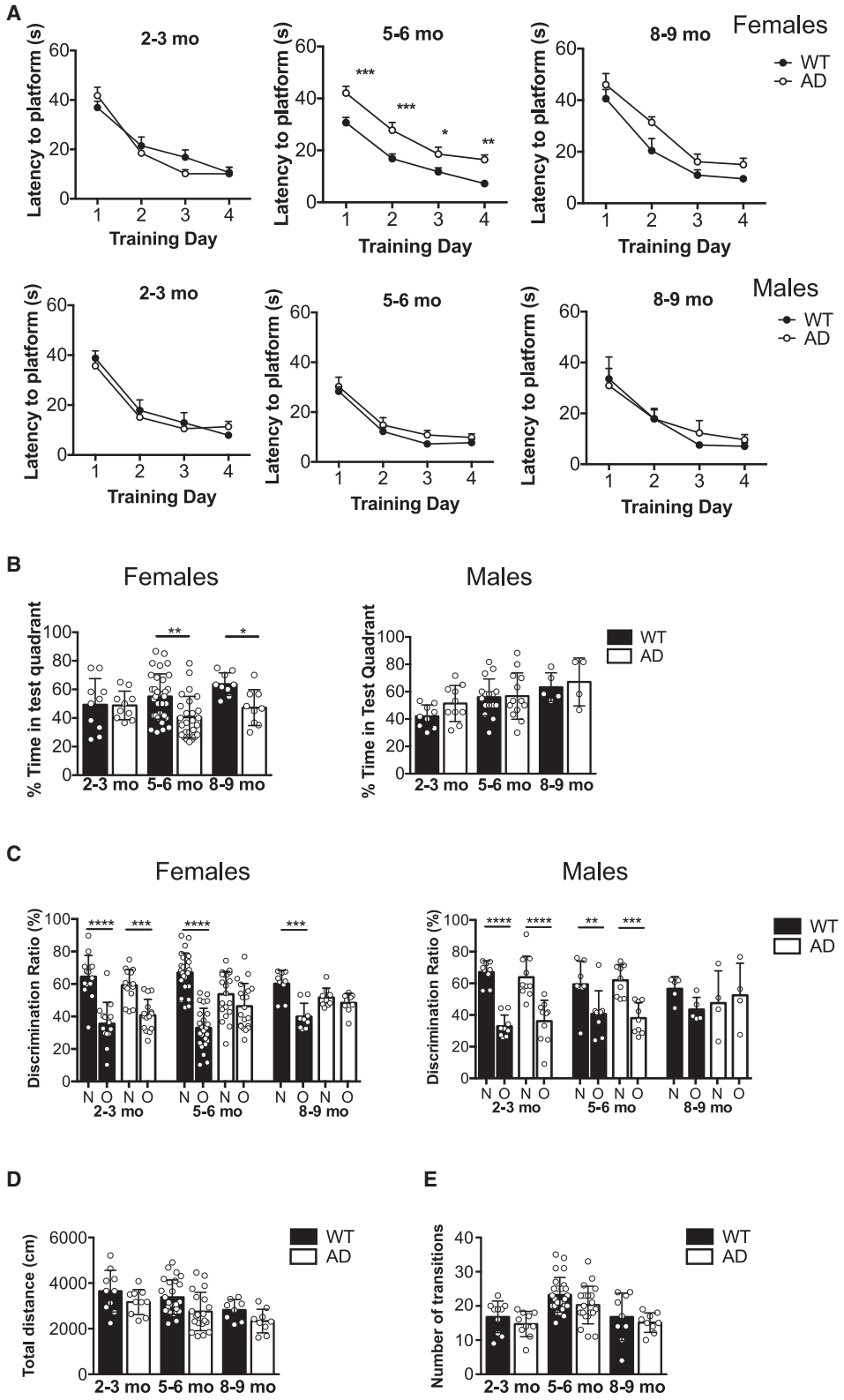

(legend on next page)

injury (Shichita et al., 2009; Sutton et al., 2009; Benakis et al., 2016), and autism-like behavior (Choi et al., 2016). In these cases, IL-17-producing cells, namely $CD4^+$ helper type 17 (Th17) and γδ (γδ17) T cells, have been pointed out as critical players in disease progression by promoting a local immune amplification loop in the meninges as well as blood-brain barrier (BBB) disruption (Shichita et al., 2009; Sutton et al., 2009; Gelderblom et al., 2012; Benakis et al., 2016). Moreover, in a rodent model of Parkinson's disease (PD), Th17 cells were described to exacerbate neuroinflammation and neurodegeneration (Liu et al., 2019), which is paralleled by elevated production of IL-17 by $CD4^+$ T cells in patients with PD (Sommer et al., 2018). Altogether, these findings suggest that IL-17 may be instrumentally involved in various neurodegenerative diseases. Accordingly, an increased proportion of circulating Th17 cells was observed in subjects with mild cognitive impairment (MCI) (Oberstein et al., 2018), and the rise of IL-17 levels in the serum of AD linked to disease progression (Chen et al., 2014). Th17 cells are reported to infiltrate the brain of AD models, promoting inflammation and neuronal death (Siffrin et al., 2010; Yang et al., 2017). In line with this, neutralization of IL-17 was shown to rescue neuroinflammation and memory impairments induced by direct Aβ administration (Cristiano et al., 2019). However, the impact of IL-17 on brain cognitive function at the onset and during the course of AD remains to be addressed.

Herein, we report a substantial increase of IL-17-producing T cells, mostly γδ T cells, in the CNS of a transgenic model of AD—3xTg-AD mice—at early stages of the disease. Interestingly, this phenotype associated with cognitive deficits observed in females, but not in males, thus translating the sexual dimorphism observed in patients with AD (Fisher et al., 2018). Importantly, anti-IL-17 monoclonal antibody (mAb) intracerebroventricular (ICV) treatment of females prevented short-term memory deficits and synaptic plasticity impairments, prior to the detection of Aβ or tau pathologies. Our data therefore strongly suggest that exacerbated levels of meningeal IL-17 promote synaptic dysfunction underlying the cognitive decline in early stages of AD.

RESULTS

$IL\text{-}17^+$ cells accumulate in the CNS at the onset of cognitive decline in 3xTg-AD mouse model

An increase of IL-17 levels in the serum has been linked to disease progression in patients with AD (Chen et al., 2014). To investigate the role of IL-17 in neuropathological changes and memory deficits associated with the early onset of AD, we used the triple-transgenic mouse model of AD (3xTg-AD), a progressive model of the disease developing both amyloid plaques and neurofibrillary tangles (Oddo et al., 2003b).

Animals were tested at an early stage (2 to 3 months old, i.e., prior to detection of any cognitive deficits), at the onset of disease (5 to 6 months old, when the cognitive deficits start), and at later stages (8 to 9 months old, when pathology and memory deficits are overt; Oddo et al., 2003a; Billings et al., 2005, 2007; Giménez-Llort et al., 2007). Short- and long-term memories were tested using the Y-maze and the Morris water maze (MWM), respectively (Ribeiro et al., 2019). Cognitive deficits evaluated in MWM were only observed in female 3xTg-AD mice starting at 5 months of age, but not in males, even at later stages (8 to 9 months old), when compared with aged- and sex-match B6129/J wild-type (WT) controls (Figures 1A and 1B), as previously reported (Oddo et al., 2003a). According to our previous evidence of IL-17 requirement for short-term memory (Ribeiro et al., 2019), but not long-term, we also assessed Y-maze performance. We found a progressive reduction in the discrimination ratio of females throughout age, starting at 5 to 6 months, whereas males were found only impaired at 8 to 9 months old (Figure 1C). Of note, when compared to age and sex-match WT controls, female 3xTg-AD mice had similar levels of motor and exploratory activity and no signs of anxiety (Figures 1D and 1E), in line with published data (Oddo et al., 2003a).

We hypothesized that IL-17 could trigger AD onset; therefore, we assessed whether changes in cognitive function would be associated with alterations on the provision of IL-17 in the CNS or in the periphery. For this, we analyzed by flow cytometry the brain, meninges, cervical lymph nodes (cLNs), and spleens of WT and 3xTg-AD mice upon disease progression (Figure 2). We found that, at the onset of memory deficits (5 to 6 months of age), the meninges, the brain, and the cLNs of female 3xTg-AD mice, but not the spleen, showed higher percentages and absolute numbers of $IL\text{-}17A^+$ cells compared with age-matched WT controls (Figures 2A–2C). These differences on $IL\text{-}17^+$ cells were maintained at later stages (8 to 9 months of old). Interestingly, in contrast to females, 3xTg-AD male mice—that did not display particular cognitive decline at 5 months of age—did not exhibit any accumulation of $IL\text{-}17^+$ cells (Figures 2B and 2C). This led us to hypothesize that exacerbated IL-17 associates with memory deficits at the onset of AD, selectively in female mice (which were used in all subsequent experiments).

Figure 1. Age-dependent sexual dimorphism in 3xTg-AD mice: only females display cognitive deficits starting at 5 months of age

WT and 3xTg-AD females and males 2 to 3 months old (n = 10–15 for female mice; n = 9–10 for male mice), 5 to 6 months old (n = 20–34 for female mice; n = 9–16 for male mice), and 8 to 9 months old (n = 8–9 for female mice; n = 4–5 for male mice) were tested in the (A and B) MWM-maze, (C) Y-maze, (D) open field, and (E) elevated plus maze.

(A) The escape latency, i.e., the time required for the mice to find and climb onto the platform, was recorded for 60 s.

(B) % time in the quadrant where the platform was evaluated, in the 60-s probe test.

(C) The discrimination ratio between novel (N) and the other (O) arm was evaluated.

(D) Animals were placed in a box for 5 min and allowed to explore, and total distance (cm) was evaluated.

(E) Anxiety was evaluated by the total number of transitions between open and closed arms.

Results are representative of 1–3 independent experiments. Error bars, mean ± SEM. $^*p < 0.05$, $^{**}p < 0.01$, and $^{***}p < 0.001$ as calculated by one-way ANOVA or t test.

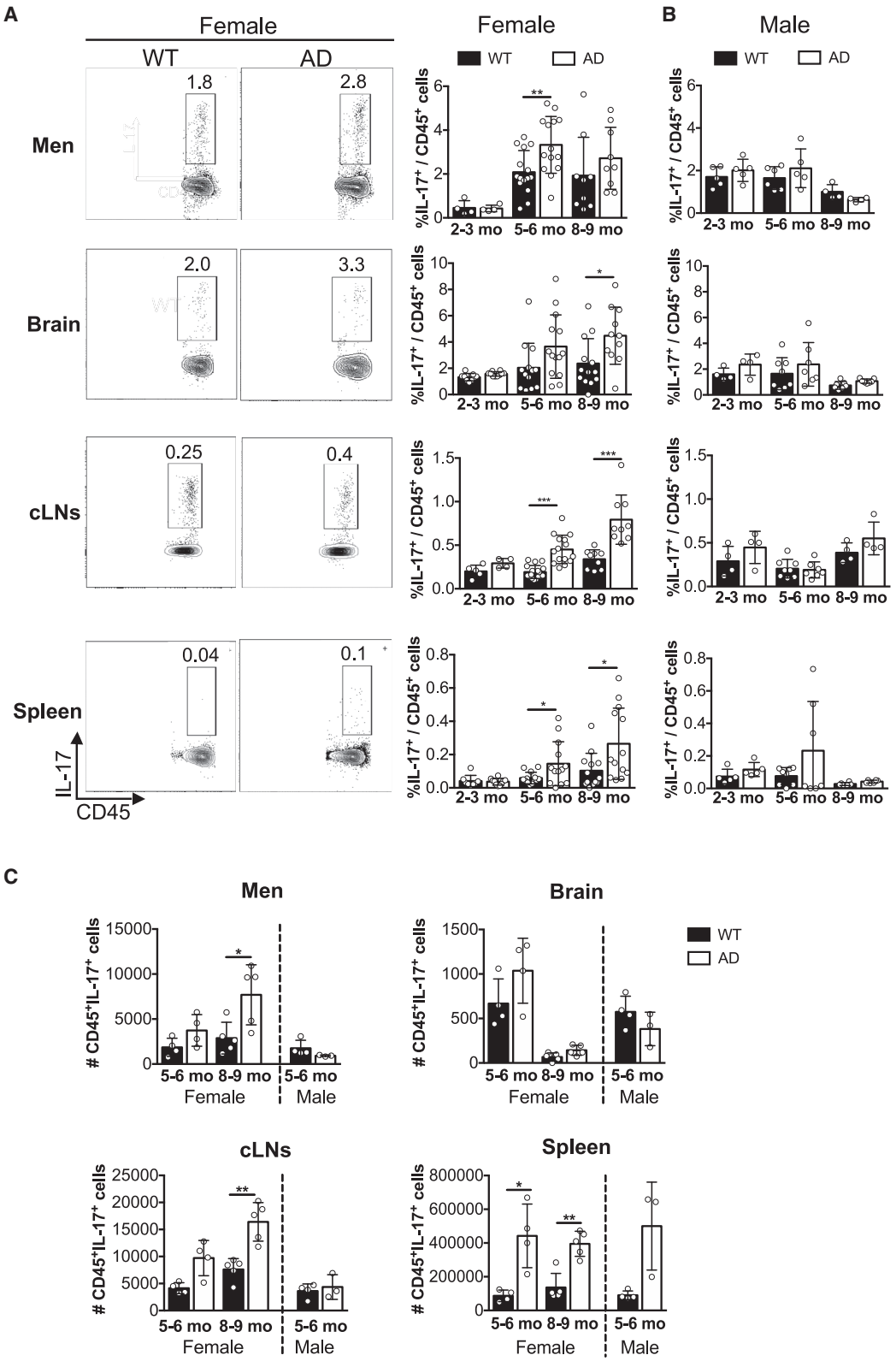

(legend on next page)

γδ T cells are the major source of IL-17 in the CNS of 3xTg-AD mice

IL-17 can be produced by $CD4^+$ T cells, $CD8^+$ T cells, γδ T cells, group 3 innate lymphoid cell (ILC3), and (natural killer) NKT cells, among other immune subsets (Hatfield and Brown, 2015; Zenaro et al., 2015; Kwong et al., 2017). In our experimental context, $CD3^+$ T cells accounted for most of the IL-17^+ $CD45^+$ cells in the meninges, brain, and cLNs of WT and AD mice (Figure 3A). In the healthy steady state, γδ T cells are known to be the main source of IL-17 in the meninges (Benakis et al., 2016; Ribeiro et al., 2019). Expectedly, IL-17 was mainly produced by γδ T cells in both WT and AD mice (Figure 3A). Also worth mentioning are other sources of meningeal IL-17, namely $CD4^+$ or $CD8^+$ T cells as well as $CD3^-$ non-T cell leukocytes, including ILC3s (Hatfield and Brown, 2015; Kwong et al., 2017) and neutrophils (Zenaro et al., 2015; Figures 3A and 3B). Accordingly to the observed accumulation of meningeal IL-17^+ cells at AD onset (Figures 2A and 2B), the percentages of γδ T cells, of IL-17^+ cells among γδ T cells, as well as the numbers of IL-17-producing γδ (γδ17) T cells were significantly higher in the meninges of 5- to 6-month-old AD mice compared with aged-matched WT controls (Figure 3B). Interestingly, this accumulation was associated with an increase of the myeloid compartment in the meninges, brain, and cLNs of AD female mice (Figures S1A and S1B). In fact, γδ T cell numbers positively correlated with the numbers of macrophages, monocytes, and neutrophils in the meninges (Figure 3C).

Of note, γδ T cells from WT and AD mice displayed a typical signature of IL-17 producers, being enriched for the expression of CCR6, RORγt, and IL-1R, when compared to their αβ counterparts, as well as a particularly activated phenotype, enriched for $CD44^{hi}$ $CD69^+$ cells (Figures S2A and S2B). Importantly, we observed a similar percentage of γδ17 T cells expressing Ki67, a marker of cell proliferation (Figure S2B). In the healthy meninges, γδ T cell receptor (TCR) repertoire is mostly restricted to gamma chain variable region 6 (Vγ6) (that was operationally defined by default as double negative for Vγ1 and Vγ4; Ribeiro et al., 2019). In EAE, CNS-infiltrating γδ17 T cells are mostly restricted to the $V\gamma4^+$ subset (Sutton et al., 2009), whereas, in models of ischemic stroke, infiltrating γδ T cells bear the Vγ6 chain (Arunachalam et al., 2017). Here, we show that the TCR repertoire of γδ17 T cells in the meninges and brain of AD mice remained highly biased for $V\gamma1^-V\gamma4^-$ (assumed as $V\gamma6^+$) subset, although $V\gamma4^+$ represented only a small fraction of total γδ17 T cells (Figure S2C).

Of note, besides meninges, brain, cLNs, and spleen, we also observed an inflammatory response of the myeloid, NK, and NKT compartments in the liver of both male and female mice (Figure S3), which was consistent with the previously described amyloidosis in this organ (Marchese et al., 2014).

IL-17 neutralization prevents short-term cognitive deficits in 3xTg-AD mice

Next, we assessed whether the exacerbated levels of IL-17 in the brain and meninges of female 3xTg-AD mice had a detrimental role on cognitive performances. For this, neutralizing anti-IL-17 mAb (anti-IL-17A; 32.5 μg/day) or isotype control IgG1a (immunoglobulin G [IgG]; 32.5 μg/day) was chronically diffused through a micro-pump delivery system into the right ventricle of 3xTg-AD and WT mice. This chronic delivery of anti-IL-17 was made for a period of 6 weeks at a rate of 0.15 μL/h starting at 3.5 months of age, prior to any detectable cognitive deficit (3.5 months old; Figure 4A). Of note, treated animals did not show any weight alteration (Figure 4B) or particular signs of locomotor impairments or anxiety, as evaluated in the open-field (OF) test or in the elevated plus maze (EPM) (Figures 4C and 4D). Strikingly, at 5 months of age, we observed that anti-IL-17-treated AD mice (AD+aIL-17) were able to discriminate between the novel and the familial arm of the Y-maze test, similarly to WT controls (WT+IgG), whereas control IgG-treated AD mice were not (Figure 4E). These data indicate that anti-IL-17 treatment prevents short-term cognitive decline observed in 5-month-old AD mice when tested in the Y-maze. Conversely, the ICV administration of 300 ng of IL-17 alone to WT mice was sufficient to induce short-term memory deficits (Figure S4A), which demonstrates the potent detrimental effects of dysregulated and exacerbated levels of IL-17 on brain cognitive functions. This notwithstanding, the long-term cognitive impairments assessed in the MWM could not be rescued by the anti-IL-17 treatment (Figures 4F and 4G). These data indicate that early intervention with neutralizing IL-17 is efficient in preventing short-term reference memory deficits, but not the long-term spatial memory defect observed in AD mice at 5 months of age.

To assess whether manipulation of IL-17 could be efficient in altering the progression of the disease until later stages, a set of 3xTg-AD mice were treated for a prolonged period, from 3.5 to 7 months of age, with either control IgG or anti-IL-17 mAb (Figure S5). We verified that the procedure did not impact on the weight, exploratory behavior, or anxiety of animals (Figures S5A–S5C). Interestingly, the anti-IL-17 treatment in the AD group resulted in preservation of short-term memory performance in the Y-maze, whereas IgG alone did not alter the impaired discrimination of AD mice (Figure S5D). Again, no differences were observed in the MWM between mice treated with either IgG or anti-IL-17 (Figures S5E and S5F). Further histological analysis of the amyloid load and of the phosphoTau levels in

Figure 2. Accumulation of IL-17^+ cells in the CNS at the onset of cognitive deficits

Meningeal (Men), brain, cervical lymph nodes (cLNs), and spleen cell suspensions were prepared from 2- to 3- (n = 4–10 for female mice; n = 4–5 for male mice), 5- to 6- (n = 4–17 for female; n = 4–8 for male mice), and 8- to 9-month-old (n = 5–14 for female; n = 4–6 for male mice) WT and 3xTg-AD female (A and C) and male (B and C) mice. Samples were analyzed for the expression of surface CD45 and intracellular IL-17 markers. Live cells were gated using LiveDead Fixable Viability Dye.

(A) Dot plots represent cell populations from indicated gates.

(B and C) Histograms depict percentages (n = 4–17 mice; B) or absolute numbers (n = 3–5 mice; C) from indicated populations.

Results are representative of 1–4 independent experiments. Error bars, mean ± SD. *$p < 0.05$, **$p < 0.01$, and ***$p < 0.001$, as calculated by Mann-Whitney or unpaired t test.

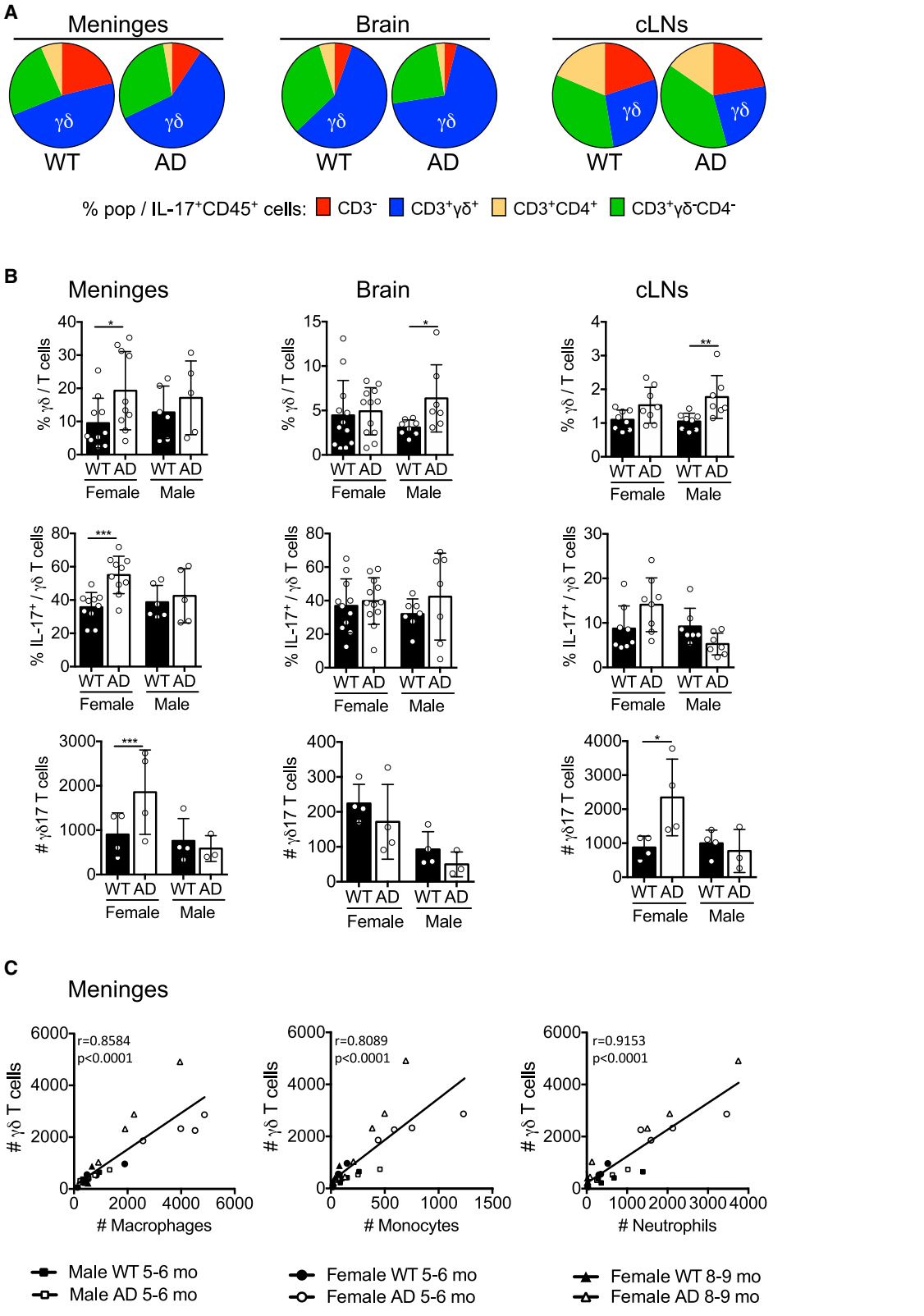

(legend on next page)

3xTg-AD showed no impact of the anti-IL-17 infusion, measured by 6E10 and AT8 antibody staining, respectively (Figure S5G). Regarding neuronal counting and microglial and astrocytic markers (Nissl, Iba1, and GFAP stainings, respectively), we only observed a slight increase in Iba1 staining upon anti-IL-17 treatment and no changes in the remaining markers. As anticipated in our previous study (Ribeiro et al., 2019), this suggests that synaptic function, rather than amyloid-related pathways, is being targeted by the IL-17-mediated regulation of cognitive behavior.

In AD mouse models, splenomegaly is a common manifestation of amyloidosis that is often accompanied by inflammation (Marchese et al., 2014; Yang et al., 2015). Interestingly, the prolonged anti-IL-17 mAb infusion was also associated with a reduced splenomegaly in AD mice (Figure S5H). We therefore propose that prolonged neutralization of IL-17 in 3xTg-AD mice delays the onset of short-term memory deficits and may have a broader impact on the AD-related inflammatory profile in the periphery, beyond the CNS.

IL-17 neutralization prevents synaptic dysfunction independently of Aβ and tau pathology or BBB disruption

To determine whether anti-IL-17 could be beneficial in the prevention of cognitive deficits by affecting AD-related pathological hallmarks, we assessed Aβ and tau pathologies by immunohistochemistry and western blot (WB) analysis (Figures 5A–5C). Immunohistochemical studies showed that 5-month-old anti-IL-17- or IgG-treated 3xTgAD mice equally accumulate mild intraneuronal amyloid precursor protein (APP), although they do not yet display Aβ plaques (Figure 5A). Also, total APP levels and C-terminal fragments were similar between AD+IgG, AD+aIL-17, and WT+IgG mice, as assessed by WB (Figure 5B). Furthermore, biochemical analysis revealed no major changes in total tau expression (N-ter and C-Ter), dephosphorylated Tau (Tau1), or phosphorylation at multiple Tau epitopes (S396, S199, S262, S404, and AT100 [Thr212 and Ser214]) of AD+IgG, AD+aIL-17 when compared with WT+IgG mice (Figure 5C). As previously reported (Oddo et al., 2003b), these data further support that disease onset, characterized by mild cognitive impairments, occurs prior to the establishment of Aβ and tau pathologies. Furthermore, we did not find any sign of BBB disruption in AD mice at this age. Upon intraperitoneal injection of Evans blue, the dye was not detected in the parenchyma of the brains of WT or AD mice, indicating that the BBB is structurally and functionally intact (Figure 5D).

We have previously described the involvement of IL-17 in hippocampal glutamatergic transmission and synaptic plasticity in physiological context (Ribeiro et al., 2019). Therefore, we next sought to address whether the same synaptic targets were deregulated in this context. To investigate basal synaptic transmission, we generated input/output (I/O) curves by recording excitatory postsynaptic potentials (fEPSPs) from the Schaffer/CA1 synapse at increasing stimulus intensities (0.8–3 mA). The I/O curve from AD+IgG mice attained a significant lower maximum value compared to WT+IgG mice (Figure 5E), as previously described (Oddo et al., 2003b), that was normalized by the anti-IL-17-chronic infusion. We further measured long-term potentiation (LTP) in the CA1 region, as a functional readout for the neural basis of learning and memory (Bliss and Collingridge, 1993). AD-IgG mice display decreased LTP when compared with WT−IgG mice, as expected (Oddo et al., 2003b). Notably, neutralization of IL-17 in AD mice diminished the LTP impairment (Figure 5F). Conversely, we observed that preincubation of IL-17 (30 ng/mL) was sufficient to significantly impair LTP, as opposed to IL-17 (10 ng/mL) that had no effect (Figure S4B). Building on our previous study (Ribeiro et al., 2019), these data suggest that IL-17 action follows a bell-shaped curve, being crucial for synaptic transmission up to a certain level, from which it becomes deleterious.

Altogether, we concluded that exacerbated levels of IL-17 induce glutamatergic synaptic dysfunction and propose that such mechanism would trigger short-term cognitive impairments in AD mice at disease onset.

DISCUSSION

The impact of immune mediators on cognitive loss associated with AD onset remains elusive (Da Mesquita et al., 2018). In the present study, we show that IL-17-producing cells, mostly γδ T cells, accumulate in the CNS at the onset of cognitive deficits and persist throughout disease progression. IL-17 neutralization was sufficient to prevent short-term memory deficits and hippocampal glutamatergic dysfunction in early stages of disease, in a mechanism that is independent of Aβ and Tau pathology or BBB disruption. In later stages of disease, prolonged anti-IL-17 infusion resulted in the delay of cognitive impairment, accompanied by a reduction in peripheral inflammation. Therefore, we propose that elevated levels of IL-17 at early stages of disease contribute to synaptic dysfunction and short-term memory deficits in the 3xTg-AD mouse model.

The role of IL-17 in early stages of Alzheimer's pathology is controversial and poorly explored. If, on one hand, neutralization of IL-17 was shown to rescue Aβ-induced neuroinflammation and memory impairments (Cristiano et al., 2019), on the other side, it is reported that IL-17A overexpression in AD mouse brain is neuroprotective, decreasing amyloid angiopathy (Yang et al.,

Figure 3. γδ T cells are a major source of IL-17 in the CNS of 3xTg-AD mice

Meningeal, brain, and cLNs cell suspensions were prepared from 5- to 6- and 8- to 9-month-old WT and 3xTg-AD female and male mice. Samples were analyzed for the expression of surface CD45, CD3, CD4, TCRδ, CD11b, F4/80, Ly6C, and Ly6G.

(A) Live cells were gated using LiveDead Fixable Viability Dye. Pie charts represent indicated cell populations from indicated gates (n = 4–11 mice).

(B) Histograms depict percentages of γδ T cell (top panels) or IL-17-producing γδ T cells (n = 5–12 mice; middle panels) and absolute number of IL-17-producing γδ T cells (γδ17 T cells; n = 3–4 mice; lower panels).

(C) Linear regression plots of the number of γδ17 T cells and macrophages, monocytes, or neutrophils.

Results are representative of 1–3 independent experiments (n = 3–5 mice). Error bars, mean ± SD. *$p < 0.05$ and **$p < 0.01$, as calculated by Mann-Whitney, unpaired t test, and Pearson correlation.

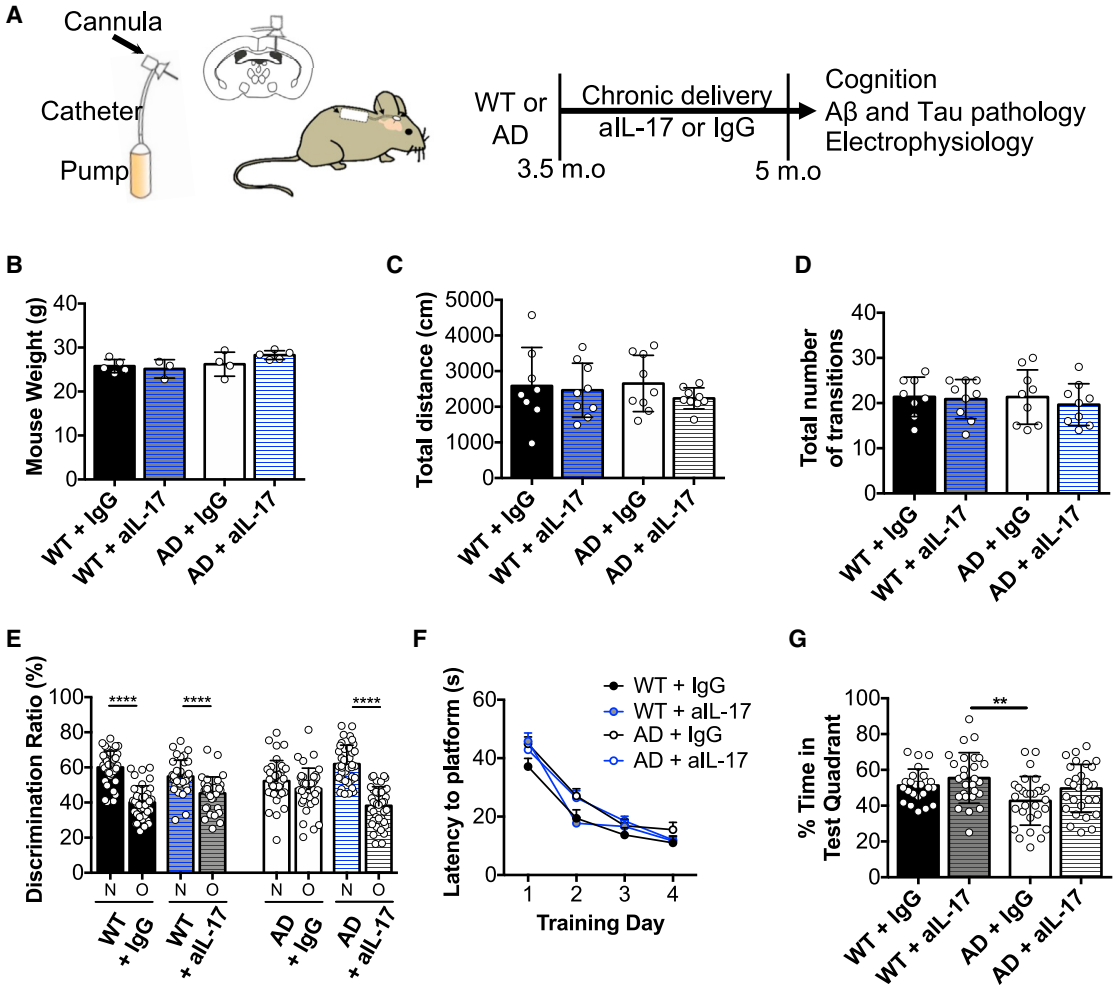

Figure 4. Early IL-17 neutralization prevents short-term cognitive deficits in 3xTg-AD mice

(A) Experimental design: WT and 3xTgAD mice were treated with either neutralizing anti-IL-17 antibody (anti-IL-17A; 32.5 μg/day) or isotype control IgG1a (IgG; 32.5 μg/day), starting at an average age of 3.5 months and continued for 6 weeks, through a micro-pump delivery system (Alzet). Cognitive assays, AD-related hallmarks (amyloid-beta [Aβ] and tau pathologies), and electrophysiology were performed after this period, in 5- to 6-month-old mice.

(B) Mouse weight in grams (g) after treatment (n = 4–5 mice).

(C) Exploratory behavior evaluated by total distance (cm) in the open field (n = 8–9 mice).

(D) Anxiety in the elevated plus evaluated by the total number of transitions between open and closed arms (n = 8–9 mice).

(E) The discrimination ratio between novel (N) and the other (O) arm was evaluated in the Y-maze test (n = 37–39 mice).

(F) Escape latency during the training phase.

(G) % time in the test quadrant where the platform was in the MWM test (n = 23–29 mice).

Results are representative of 1–6 independent experiments. Error bars, mean ± SEM. **p < 0.01 and ****p < 0.0001, as calculated by one-way ANOVA or t test.

2017). To tackle this question, we took advantage of the triple-transgenic mouse model of AD (3xTg-AD), a progressive model that allows individualizing the different stages of the disease, regarding both cognitive deficits and AD hallmarks. Importantly, it also translates the sexual dimorphism observed in humans, where women are more affected than men in both disease prevalence and symptom progression (reviewed in Fisher et al., 2018).

IL-17 is a recent player in neurophysiology linked to cognitive behavior and anxiety in mice (Ribeiro et al., 2019; Alves de Lima et al., 2020) and described as a neuromodulator of sensory responses in worms (Chen et al., 2017). Here, we show that IL-17-producing cells accumulate in the meninges and in the brain at early stages of the disease, suggesting that AD-related immune alterations might initiate at the onset of cognitive symptoms. In pathology, IL-17 is largely described to mediate inflammation of the CNS (Shichita et al., 2009; Sutton et al., 2009; Gelderblom et al., 2012; Benakis et al., 2016) and was suggested to play a role in AD and PD pathology (Zenaro et al., 2015). More recently, IL-17$^+$ CD4$^+$ (Th17) cells were described to exacerbate neuroinflammation and neurodegeneration in rodent models of PD. In the same line, elevated production of IL-17 by CD4$^+$

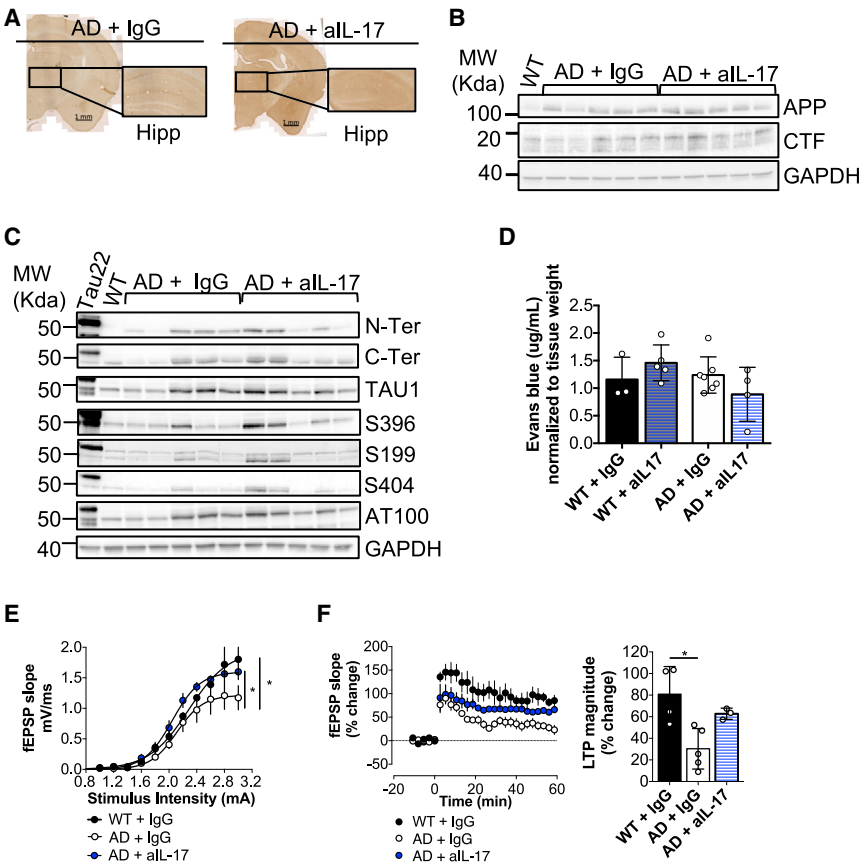

Figure 5. IL-17 neutralization prevents synaptic dysfunction independently of Aβ and tau pathology or BBB disruption

(A) Brain sections from AD+IgG and AD+aIL-17 immunostained with 6E10 antibody amplification of hippocampal region of each brain section (n = 3). Scale bars, 1 mm.

(B) Western blot (WB) of APP and C-terminal fragments (CTFs) normalized to GAPDH on the hippocampus of WT+IgG, AD+IgG, and AD+aIL-17 (n = 5 mice).

(C) WB of tau (N-ter and C-ter) and tau phosphorylation at S396, S199, S404, and S212/T214 (AT100) epitopes, as well as dephosphorylated tau (tau-1) in the hippocampus of 9-month-old Tau22 mice, as positive control, WT+IgG, AD+IgG, and AD+aIL-17 animals (n = 5 mice).

(D) Quantitative analysis of Evans blue leakage into the brain (μg/mL) normalized to tissue weight (n = 3–7 mice).

(E) Input/output (I/O) curves corresponding to the fEPSP slope evoked by different stimulation intensities (0.8–3.0 mA) of WT+IgG, AD+IgG, and AD+aIL-17; n = 3–6 mice; F-test.

(F) Time course (left panels) and magnitude (right panels) of LTP induced by theta-burst stimulation (TBS) in hippocampal slices from WT+IgG, AD+IgG, and AD+aIL-17 animals (n = 3–5 mice). Kruskal-Wallis test followed by Dunn's multiple comparisons test is shown.

Data are mean ± SD. *p < 0.05.

T cells was also reported in the PD population (Sommer et al., 2018). Although scarce, there is increasing evidence of the involvement of Th17 cells in patients with AD (Saresella et al., 2011; Oberstein et al., 2018) as well as in rodent models (Zhang et al., 2013; Cristiano et al., 2019). On the other hand, in mice subjected to EAE, a multiple sclerosis model, IL-17-producing cells—such as γδ T cells, Th17 cells, and ILC3—infiltrate the meninges and the brain and, in concert action, amplify a detrimental immune response in CNS (Sutton et al., 2009; Hatfield and Brown, 2015; reviewed in Waisman et al., 2015). We unveil that γδ T cells, followed by $CD3^+CD4^-\gamma\delta^-$ T cells, inferred to be $CD8^+$ T cells, are the major sources of IL-17 increasing in AD context. In AD, the detrimental role of $CD8^+$ T cells is mostly correlated with Tau pathology—but not amyloid pathology—in both humans (Merlini et al., 2018) and rodent models (Laurent et al., 2017). However, tissue-resident $CD8^+$ T cells were described to populate the human healthy brain, contributing to immune surveillance (Smolders et al., 2018) and to expand in the cerebrospinal fluid (CSF) of patients with AD (Gate et al., 2020). Altogether, this suggests a potential proinflammatory role of these cells in early stages of AD.

γδ T cells are reported to be impaired in elderly subjects (Colonna-Romano et al., 2004), and upon aging, there is an increased differentiation of T cell into Th17 pathway (Lee et al., 2011; Li et al., 2017). Upon aging, the main risk factor for AD, there is an increase of inflammatory cytokines, such as IL-17, as well as cytokines driving IL-17 secretion, namely IL-1 and IL-23 (Chen et al., 2014; Lim et al., 2014; Barrientos et al., 2015). Of note, we observed an increased expression of the receptor for IL-1 in meningeal γδ T cells, when compared to their αβ T cell counterparts, suggesting a potential contribution of this cytokine in the accumulation of γδ17 T cells in AD mice. In aged mice, IL-17-producing γδ T cells were shown to dominate the γδ T cell pool on lymph node, mainly due to the selective increase of $V\gamma6^+$ γδ17 T cells (Chen et al., 2019). Altogether, these data are consistent with increased circulation of Th17 cells (Saresella et al., 2011; Oberstein et al., 2018) and IL-17 levels in the serum of patients with AD (Chen et al., 2014; Hamdan et al., 2014). In addition, it has been recently reported that, upon aging and in AD models, there is an impairment in brain drainage due to the disruption of the lymphatic vessels, where immune cells reside (Da Mesquita et al., 2018; Ahn et al., 2019). This phenomenon can lead to a breakdown in the homeostasis and circulation of meningeal immune population and may underlie the elevated pool of $IL\text{-}17^+$ cells observed in our study.

To clarify whether IL-17 could contribute to the initial phase of memory impairment, we neutralized IL-17 before the onset of cognitive deficits, from 3.5-month-old to 5-month-old AD mice. Anti-IL-17 treatment was sufficient to prevent the short-term cognitive deficits observed in the onset of disease in AD models. However, the cognitive deficits in the MWM could not be prevented by the treatment. These go in line with the absence of

role of IL-17 in MWM at steady state, suggesting that other AD-related mechanisms independent of IL-17 signaling might be in place. For instance, MWM was shown to be dependent on the presence of IL-4$^+$ CD4 T cells (Derecki et al., 2010).

The role of IL-17 in AD has been so far described in the context of established Aβ pathology (Zhang et al., 2013; Cristiano et al., 2019). Here, we unveil an early role for IL-17 in AD that precedes the formation Aβ plaques, tau pathology, and BBB disruption, key features of AD. This further supports the involvement of IL-17 in initial stages of the disease. We also show that prolonged treatment with anti-IL-17 prevents the appearance of short-term cognitive deficits in later stages of disease (7 to 8 months old), suggesting that IL-17 is a triggering event in AD. We hypothesize that an accumulation of meningeal IL-17 may initiate the inflammatory cascade in the brain as well as leukocyte recruitment. Because the BBB is still intact at 5 to 6 months old, cerebral infiltration may occur through the choroid plexus (Bouzerar et al., 2013). IL-17 is a strong chemoattract of neutrophils, which are described to accumulate at the onset of cognitive deficits in the same AD model promoting AD-related pathology (Zenaro et al., 2015). Consistently, we observed a positive correlation between the absolute numbers of γδ T cells and neutrophils in the meninges, pointing at a potential cross-talk between these two populations upon disease onset, as previously reported in the context of infection (Nakasone et al., 2007; Shibata et al., 2007; Hamada et al., 2008). Neutrophils may act as perpetuators of neuronal damage following initiation of neuroinflammation downstream of IL-17 elevations. It is plausible that neutralization of IL-17 might constrain the recruitment of these and other populations into the CNS. This was previously shown in the pathogenesis of cerebral ischemia upon γδ17 T cell infiltration (Shichita et al., 2009). Anti-IL-17 treatment after stroke blocked neutrophil invasion into the brain (Gelderblom et al., 2012). In addition, γδ17 T cells are reported to amplify Th17 responses (Sutton et al., 2009; Pikor et al., 2015). This could explain why the deleterious role of Th17 cells is only described when AD pathology is fully established.

IL-17 can act directly on interneurons (Chen et al., 2017) and cortical glutamatergic neurons (Alves de Lima et al., 2020), as well as indirectly on glial cells, amplifying neuronal responses through the promotion of brain-derived neurotrophic factor (BDNF) production in the steady state (Ribeiro et al., 2019). Of note, the characterization of BDNF in AD has been largely covered (Tapia-Arancibia et al., 2008), namely in the 3xTg-AD model where BDNF signaling pathway has been shown to be impaired (Corona et al., 2010). This highlights the complexity of BDNF regulation upon neurodegeneration, implying additional and different mechanisms than the one involved at steady state.

Mechanistically, synaptic dysfunction is described to underlie the cognitive deficits observed in 3xTg-AD mice (Oddo et al., 2003b). Here, we demonstrate that anti-IL-17 treatment prevented synaptic deficits observed in basal transmission and long-term potentiation at the onset of short-term cognitive deficits of AD mice. These data suggest that exacerbated levels of IL-17 are detrimental for synaptic signaling, mirroring the findings for other cytokines, such as IL-1β and tumor necrosis factor alpha (TNF-α), involved in both homeostatic synaptic plasticity and pathology (Avital et al., 2003; Stellwagen and Malenka, 2006; Ren et al., 2011; Pribiag and Stellwagen, 2013; Prieto et al., 2015). Of note, exacerbated levels of IL-17 were shown to promote gliosis in several different settings (Sarma et al., 2009; Zimmermann et al., 2013; You et al., 2017). On the other hand, we have recently shown that IL-17 promotes synaptic plasticity and short-term memory in the physiological context, by modulating AMPA/NMDA ratio of glutamatergic synapses (Ribeiro et al., 2019). Adding to these findings, this study suggests that IL-17 can mediate opposite effects, seemingly depending on its concentration in the microenvironment, and implies a dual role for IL-17, supporting the idea that IL-17 action follows a bell-shaped curve with a threshold above which IL-17 promotes a deleterious neuroinflammation. Thus, a relevant open question remains as "how much of IL-17 is too much?". In an attempt to address this issue, we have titrated the supplementation of IL-17 in hippocampal slices of WT mice, using electrophysiology as a readout, and observed that a preincubation of 30 ng/mL of IL-17 was sufficient to significantly impair LTP, as opposed to a dose 10 ng/mL that had no effect. Of note, this concentration range is in accordance with our previous observation that 10 ng/mL was able to partially rescue LTP in IL-17 knockout (KO) mice (Ribeiro et al., 2019). Consistently, for proof of concept, we could phenocopy the mild cognitive impairment observed in AD mice by injecting a high dose of IL-17 (300 ng/mL) in the brain ventricle of WT mice.

In conclusion, we have described a pathogenic role of IL-17 in promoting synaptic dysfunction and cognitive function underlying the onset of AD. Given the pro-cognitive role of IL-17 in healthy meninges (Ribeiro et al., 2019), our data suggest that IL-17 levels are finely tuned to foster cognition in the steady state, but their pathophysiological dysregulation promotes neurodegeneration. These findings shed light in the early events driving AD pathogenesis, opening perspectives for early biomarkers of disease and combinatorial treatments where the core pathologies (Aβ plaques and tau pathology) and underlying inflammation are collectively targeted to halt the disease.

STAR★METHODS

Detailed methods are provided in the online version of this paper and include the following:

- KEY RESOURCES TABLE
- RESOURCE AVAILABILITY
  - Lead contact
  - Materials availability
  - Data and code availability
- EXPERIMENTAL MODEL AND SUBJECT DETAILS
  - Ethics statement
  - Mice
- METHOD DETAILS
  - Behavioral Tests
  - OF
  - EPM
  - Y-Maze
  - MWM
  - Surgical procedures
  - Flow cytometry

- Immunohistochemistry
- Evans Blue Quantification
- ELISA Measurements
- Western Blots
- Electrophysiological fEPSPs recordings

- QUANTIFICATION AND STATISTICAL ANALYSIS

SUPPLEMENTAL INFORMATION

Supplemental information can be found online at https://doi.org/10.1016/j.celrep.2021.109574.

ACKNOWLEDGMENTS

We thank the assistance of the staff of the Flow Cytometry and Rodent facilities of iMM Lisboa. We also thank Alexandre de Mendonça, Margarida Correia Neves, and Nuno Morais for helpful discussions and technical support. This work was funded by the Fundação para a Ciência e Tecnologia (IF/00013/2014, LISBOA-01-0145-FEDER-028241, and PTDC/MED-IMU/1988/2020) to J.C.R., Santa Casa da Misericórdia (MB-7-2018) and Fundacão para a Ciência e Tecnologia (PTDC/BIM-MEC/4778/2014 and IF/00105/2012) to L.V.L., and PD/BD/114103/2015 to H.C.B. The ORCIDs for this article are as follows: 0000-0001-8367-3005 (L.V.L.) and 0000-0002-7852-343X (J.C.R.).

AUTHOR CONTRIBUTIONS

H.C.B. designed and performed the experiments and analyzed the data, except when otherwise stated, and wrote the manuscript. M.R., J.E.C., S.C.-P., J. Darrigues, J. Dunot, H.M., and A.A.d.A. assisted in some experiments of flow cytometry, electrophysiology, ICV injection, and behavioral tests. R.G. assisted in RNA extraction and RT-PCR experiments, and S.C.-P. assisted in experiments of immune-cell isolation. Histology and western blot experiments were performed by H.C.B. at the University of Lille, INSERM – Lille France, in a PhD exchange period with assistance and collaboration of D.B., E.F., V.G.-M., and K.C. P.A.P. and B.S.-S. assisted in the experimental design and provided key research tools; L.V.L. and J.C.R. coordinated the study, performed some experiments, supervised the research, and wrote the manuscript.

DECLARATION OF INTERESTS

The authors declare no competing interest.

Received: August 27, 2020
Revised: June 9, 2021
Accepted: July 30, 2021
Published: August 24, 2021

REFERENCES

Ahn, J.H., Cho, H., Kim, J.H., Kim, S.H., Ham, J.S., Park, I., Suh, S.H., Hong, S.P., Song, J.H., Hong, Y.K., et al. (2019). Meningeal lymphatic vessels at the skull base drain cerebrospinal fluid. Nature *572*, 62–66.

Alves de Lima, K., Rustenhoven, J., Da Mesquita, S., Wall, M., Salvador, A.F., Smirnov, I., Martelossi Cebinelli, G., Mamuladze, T., Baker, W., Papadopoulos, Z., et al. (2020). Meningeal γδ T cells regulate anxiety-like behavior via IL-17a signaling in neurons. Nat. Immunol. *21*, 1421–1429.

Arunachalam, P., Ludewig, P., Melich, P., Arumugam, T.V., Gerloff, C., Prinz, I., Magnus, T., and Gelderblom, M. (2017). CCR6 (CC chemokine receptor 6) is essential for the migration of detrimental natural interleukin-17-producing γδ T cells in stroke. Stroke *48*, 1957–1965.

Aspelund, A., Antila, S., Proulx, S.T., Karlsen, T.V., Karaman, S., Detmar, M., Wiig, H., and Alitalo, K. (2015). A dural lymphatic vascular system that drains brain interstitial fluid and macromolecules. J. Exp. Med. *212*, 991–999.

Avital, A., Goshen, I., Kamsler, A., Segal, M., Iverfeldt, K., Richter-Levin, G., and Yirmiya, R. (2003). Impaired interleukin-1 signaling is associated with deficits in hippocampal memory processes and neural plasticity. Hippocampus *13*, 826–834.

Barrientos, R.M., Kitt, M.M., Watkins, L.R., and Maier, S.F. (2015). Neuroinflammation in the normal aging hippocampus. Neuroscience *309*, 84–99.

Benakis, C., Brea, D., Caballero, S., Faraco, G., Moore, J., Murphy, M., Sita, G., Racchumi, G., Ling, L., Pamer, E.G., et al. (2016). Commensal microbiota affects ischemic stroke outcome by regulating intestinal γδ T cells. Nat. Med. *22*, 516–523.

Billings, L.M., Oddo, S., Green, K.N., McGaugh, J.L., and LaFerla, F.M. (2005). Intraneuronal Abeta causes the onset of early Alzheimer's disease-related cognitive deficits in transgenic mice. Neuron *45*, 675–688.

Billings, L.M., Green, K.N., McGaugh, J.L., and LaFerla, F.M. (2007). Learning decreases A β*56 and tau pathology and ameliorates behavioral decline in 3xTg-AD mice. J. Neurosci. *27*, 751–761.

Bliss, T.V.P., and Collingridge, G.L. (1993). A synaptic model of memory: long-term potentiation in the hippocampus. Nature *361*, 31–39.

Bouzerar, R., Chaarani, B., Gondry-Jouet, C., Zmudka, J., and Balédent, O. (2013). Measurement of choroid plexus perfusion using dynamic susceptibility MR imaging: capillary permeability and age-related changes. Neuroradiology *55*, 1447–1454.

Chen, J.M., Jiang, G.X., Li, Q.W., Zhou, Z.M., and Cheng, Q. (2014). Increased serum levels of interleukin-18, -23 and -17 in Chinese patients with Alzheimer's disease. Dement. Geriatr. Cogn. Disord. *38*, 321–329.

Chen, C., Itakura, E., Nelson, G.M., Sheng, M., Laurent, P., Fenk, L.A., Butcher, R.A., Hegde, R.S., and de Bono, M. (2017). IL-17 is a neuromodulator of Caenorhabditis elegans sensory responses. Nature *542*, 43–48.

Chen, H.C., Eling, N., Martinez-Jimenez, C.P., O'Brien, L.M., Carbonaro, V., Marioni, J.C., Odom, D.T., and de la Roche, M. (2019). IL-7-dependent compositional changes within the γδ T cell pool in lymph nodes during ageing lead to an unbalanced anti-tumour response. EMBO Rep. *20*, e47379.

Choi, G.B., Yim, Y.S., Wong, H., Kim, S., Kim, H., Kim, S.V., Hoeffer, C.A., Littman, D.R., and Huh, J.R. (2016). The maternal interleukin-17a pathway in mice promotes autism-like phenotypes in offspring. Science *351*, 933–999.

Coelho, J.E., Alves, P., Canas, P.M., Valadas, J.S., Shmidt, T., Batalha, V.L., Ferreira, D.G., Ribeiro, J.A., Bader, M., Cunha, R.A., et al. (2014). Overexpression of adenosine A2A receptors in rats: effects on depression, locomotion, and anxiety. Front. Psychiatry *5*, 67.

Colonna-Romano, G., Aquino, A., Bulati, M., Lio, D., Candore, G., Oddo, G., Scialabba, G., Vitello, S., and Caruso, C. (2004). Impairment of gamma/delta T lymphocytes in elderly: implications for immunosenescence. Exp. Gerontol. *39*, 1439–1446.

Corona, C., Masciopinto, F., Silvestri, E., Viscovo, A.D., Lattanzio, R., Sorda, R.L., Ciavardelli, D., Goglia, F., Piantelli, M., Canzoniero, L.M.T., and Sensi, S.L. (2010). Dietary zinc supplementation of 3xTg-AD mice increases BDNF levels and prevents cognitive deficits as well as mitochondrial dysfunction. Cell Death Dis. *1*, e91.

Cristiano, C., Volpicelli, F., Lippiello, P., Buono, B., Raucci, F., Piccolo, M., Iqbal, A.J., Irace, C., Miniaci, M.C., Perrone Capano, C., et al. (2019). Neutralization of IL-17 rescues amyloid-β-induced neuroinflammation and memory impairment. Br. J. Pharmacol. *176*, 3544–3557.

Da Mesquita, S., Louveau, A., Vaccari, A., Smirnov, I., Cornelison, R.C., Kingsmore, K.M., Contarino, C., Onengut-Gumuscu, S., Farber, E., Raper, D., et al. (2018). Functional aspects of meningeal lymphatics in ageing and Alzheimer's disease. Nature *560*, 185–191.

Da Mesquita, S., Papadopoulos, Z., Dykstra, T., Brase, L., Farias, F.G., Wall, M., Jiang, H., Kodira, C.D., de Lima, K.A., Herz, J., et al.; Dominantly Inherited Alzheimer Network (2021). Meningeal lymphatics affect microglia responses and anti-Aβ immunotherapy. Nature *593*, 255–260.

Derecki, N.C., Cardani, A.N., Yang, C.H., Quinnies, K.M., Crihfield, A., Lynch, K.R., and Kipnis, J. (2010). Regulation of learning and memory by meningeal immunity: a key role for IL-4. J. Exp. Med. *207*, 1067–1080.

Dubois, B., Feldman, H.H., Jacova, C., Cummings, J.L., Dekosky, S.T., Barberger-Gateau, P., Delacourte, A., Frisoni, G., Fox, N.C., Galasko, D., et al. (2010). Revising the definition of Alzheimer's disease: a new lexicon. Lancet Neurol. *9*, 1118–1127.

Filiano, A.J., Xu, Y., Tustison, N.J., Marsh, R.L., Baker, W., Smirnov, I., Overall, C.C., Gadani, S.P., Turner, S.D., Weng, Z., et al. (2016). Unexpected role of interferon-γ in regulating neuronal connectivity and social behaviour. Nature *535*, 425–429.

Fisher, D.W., Bennett, D.A., and Dong, H. (2018). Sexual dimorphism in predisposition to Alzheimer's disease. Neurobiol. Aging *70*, 308–324.

Gadani, S.P., Smirnov, I., Smith, A.T., Overall, C.C., and Kipnis, J. (2017). Characterization of meningeal type 2 innate lymphocytes and their response to CNS injury. J. Exp. Med. *214*, 285–296.

Gate, D., Saligrama, N., Leventhal, O., Yang, A.C., Unger, M.S., Middeldorp, J., Chen, K., Lehallier, B., Channappa, D., De Los Santos, M.B., et al. (2020). Clonally expanded CD8 T cells patrol the cerebrospinal fluid in Alzheimer's disease. Nature *577*, 399–404.

Gelderblom, M., Weymar, A., Bernreuther, C., Velden, J., Arunachalam, P., Steinbach, K., Orthey, E., Arumugam, T.V., Leypoldt, F., Simova, O., et al. (2012). Neutralization of the IL-17 axis diminishes neutrophil invasion and protects from ischemic stroke. Blood *120*, 3793–3802.

Giménez-Llort, L., Blázquez, G., Cañete, T., Johansson, B., Oddo, S., Tobeña, A., LaFerla, F.M., and Fernández-Teruel, A. (2007). Modeling behavioral and neuronal symptoms of Alzheimer's disease in mice: a role for intraneuronal amyloid. Neurosci. Biobehav. Rev. *31*, 125–147.

Hamada, S., Umemura, M., Shiono, T., Tanaka, K., Yahagi, A., Begum, M.D., Oshiro, K., Okamoto, Y., Watanabe, H., Kawakami, K., et al. (2008). IL-17A produced by gammadelta T cells plays a critical role in innate immunity against listeria monocytogenes infection in the liver. J. Immunol. *181*, 3456–3463.

Hamdan, A.A., Melconian, A.K., Adhia, A.H., and Alhaidary, A.F. (2014). The level of IL- 1α, IL-10 and IL-17A in Alzheimer's disease patients: comparative study. Baghdad Sci. J. *11*, 1486–1492.

Hatfield, J.K., and Brown, M.A. (2015). Group 3 innate lymphoid cells accumulate and exhibit disease-induced activation in the meninges in EAE. Cell. Immunol. *297*, 69–79.

Korin, B., Ben-Shaanan, T.L., Schiller, M., Dubovik, T., Azulay-Debby, H., Boshnak, N.T., Koren, T., and Rolls, A. (2017). High-dimensional, single-cell characterization of the brain's immune compartment. Nat. Neurosci. *20*, 1300–1309.

Kwong, B., Rua, R., Gao, Y., Flickinger, J., Jr., Wang, Y., Kruhlak, M.J., Zhu, J., Vivier, E., McGavern, D.B., and Lazarevic, V. (2017). T-bet-dependent NKp46^{+} innate lymphoid cells regulate the onset of T_H17-induced neuroinflammation. Nat. Immunol. *18*, 1117–1127.

Laurent, C., Dorothée, G., Hunot, S., Martin, E., Monnet, Y., Duchamp, M., Dong, Y., Légeron, F.P., Leboucher, A., Burnouf, S., et al. (2017). Hippocampal T cell infiltration promotes neuroinflammation and cognitive decline in a mouse model of tauopathy. Brain *140*, 184–200.

Lee, J.S., Lee, W.W., Kim, S.H., Kang, Y., Lee, N., Shin, M.S., Kang, S.W., and Kang, I. (2011). Age-associated alteration in naive and memory Th17 cell response in humans. Clin. Immunol. *140*, 84–91.

Li, Q., Ding, S., Wang, Y.M., Xu, X., Shen, Z., Fu, R., Liu, M., Hu, C., Zhang, C., Cao, Q., and Wang, Y. (2017). Age-associated alteration in Th17 cell response is related to endothelial cell senescence and atherosclerotic cerebral infarction. Am. J. Transl. Res. *9*, 5160–5168.

Lim, M.A., Lee, J., Park, J.S., Jhun, J.Y., Moon, Y.M., Cho, M.L., and Kim, H.Y. (2014). Increased Th17 differentiation in aged mice is significantly associated with high IL-1β level and low IL-2 expression. Exp. Gerontol. *49*, 55–62.

Lin, Y., Zhang, J.C., Yao, C.Y., Wu, Y., Abdelgawad, A.F., Yao, S.L., and Yuan, S.Y. (2016). Critical role of astrocytic interleukin-17 A in post-stroke survival and neuronal differentiation of neural precursor cells in adult mice. Cell Death Dis. *7*, e2273.

Liu, Z., Qiu, A.W., Huang, Y., Yang, Y., Chen, J.N., Gu, T.T., Cao, B.B., Qiu, Y.H., and Peng, Y.P. (2019). IL-17A exacerbates neuroinflammation and neurodegeneration by activating microglia in rodent models of Parkinson's disease. Brain Behav. Immun. *81*, 630–645.

Louveau, A., Smirnov, I., Keyes, T.J., Eccles, J.D., Rouhani, S.J., Peske, J.D., Derecki, N.C., Castle, D., Mandell, J.W., Lee, K.S., et al. (2015). Structural and functional features of central nervous system lymphatic vessels. Nature *523*, 337–341.

Marchese, M., Cowan, D., Head, E., Ma, D., Karimi, K., Ashthorpe, V., Kapadia, M., Zhao, H., Davis, P., and Sakic, B. (2014). Autoimmune manifestations in the 3xTg-AD model of Alzheimer's disease. J. Alzheimers Dis. *39*, 191–210.

Merlini, M., Kirabali, T., Kulic, L., Nitsch, R.M., and Ferretti, M.T. (2018). Extravascular CD3+ T cells in brains of Alzheimer disease patients correlate with Tau but not with amyloid pathology: an immunohistochemical study. Neurodegener. Dis. *18*, 49–56.

Monteiro, S., Ferreira, F.M., Pinto, V., Roque, S., Morais, M., de Sá Calçada, D., Mota, C., Correia-Neves, M., and Cerqueira, J.J. (2016). Absence of IFNγ promotes hippocampal plasticity and enhances cognitive performance. Transl. Psychiatry *6*, e707.

Nakasone, C., Yamamoto, N., Nakamatsu, M., Kinjo, T., Miyagi, K., Uezu, K., Nakamura, K., Higa, F., Ishikawa, H., O'brien, R.L., et al. (2007). Accumulation of gamma/delta T cells in the lungs and their roles in neutrophil-mediated host defense against pneumococcal infection. Microbes Infect. *9*, 251–258.

Oberstein, T.J., Taha, L., Spitzer, P., Hellstern, J., Herrmann, M., Kornhuber, J., and Maler, J.M. (2018). Imbalance of circulating Th17 and regulatory T cells in Alzheimer's disease: a case control study. Front. Immunol. *9*, 1213.

Oddo, S., Caccamo, A., Kitazawa, M., Tseng, B.P., and LaFerla, F.M. (2003). Amyloid deposition precedes tangle formation in a triple transgenic model of Alzheimer's disease. Neurobiol. Aging *24*, 1063–1070.

Oddo, S., Caccamo, A., Shepherd, J.D., Murphy, M.P., Golde, T.E., Kayed, R., Metherate, R., Mattson, M.P., Akbari, Y., and LaFerla, F.M. (2003). Triple-transgenic model of Alzheimer's disease with plaques and tangles: intracellular Abeta and synaptic dysfunction. Neuron *39*, 409–421.

Pikor, N.B., Astarita, J.L., Summers-Deluca, L., Galicia, G., Qu, J., Ward, L.A., Armstrong, S., Dominguez, C.X., Malhotra, D., Heiden, B., et al. (2015). Integration of Th17- and lymphotoxin-derived signals initiates meningeal-resident stromal cell remodeling to propagate neuroinflammation. Immunity *43*, 1160–1173.

Pribiag, H., and Stellwagen, D. (2013). TNF-α downregulates inhibitory neurotransmission through protein phosphatase 1-dependent trafficking of GABA(A) receptors. J. Neurosci. *33*, 15879–15893.

Prieto, G.A., Snigdha, S., Baglietto-Vargas, D., Smith, E.D., Berchtold, N.C., Tong, L., Ajami, D., LaFerla, F.M., Rebek, J., Jr., and Cotman, C.W. (2015). Synapse-specific IL-1 receptor subunit reconfiguration augments vulnerability to IL-1β in the aged hippocampus. Proc. Natl. Acad. Sci. USA *112*, E5078–E5087.

Reitz, C., and Mayeux, R. (2014). Alzheimer disease: epidemiology, diagnostic criteria, risk factors and biomarkers. Biochem. Pharmacol. *88*, 640–651.

Ren, W.J., Liu, Y., Zhou, L.J., Li, W., Zhong, Y., Pang, R.P., Xin, W.J., Wei, X.H., Wang, J., Zhu, H.Q., et al. (2011). Peripheral nerve injury leads to working memory deficits and dysfunction of the hippocampus by upregulation of TNF-α in rodents. Neuropsychopharmacology *36*, 979–992.

Ribeiro, M., Brigas, H.C., Temido-Ferreira, M., Pousinha, P.A., Regen, T., Santa, C., Coelho, J.E., Marques-Morgado, I., Valente, C.A., Omenetti, S., et al. (2019). Meningeal γδ T cell-derived IL-17 controls synaptic plasticity and short-term memory. Sci. Immunol. *4*, eaay5199.

Saresella, M., Calabrese, E., Marventano, I., Piancone, F., Gatti, A., Alberoni, M., Nemni, R., and Clerici, M. (2011). Increased activity of Th-17 and Th-9 lymphocytes and a skewing of the post-thymic differentiation pathway are seen in Alzheimer's disease. Brain Behav. Immun. *25*, 539–547.

Sarma, J.D., Ciric, B., Marek, R., Sadhukhan, S., Caruso, M.L., Shafagh, J., Fitzgerald, D.C., Shindler, K.S., and Rostami, A. (2009). Functional interleukin-17 receptor A is expressed in central nervous system glia and upregulated in experimental autoimmune encephalomyelitis. J. Neuroinflammation *6*, 14.

Shibata, K., Yamada, H., Hara, H., Kishihara, K., and Yoshikai, Y. (2007). Resident Vdelta1+ gammadelta T cells control early infiltration of neutrophils after Escherichia coli infection via IL-17 production. J. Immunol. *178*, 4466–4472.

Shichita, T., Sugiyama, Y., Ooboshi, H., Sugimori, H., Nakagawa, R., Takada, I., Iwaki, T., Okada, Y., Iida, M., Cua, D.J., et al. (2009). Pivotal role of cerebral interleukin-17-producing gammadeltaT cells in the delayed phase of ischemic brain injury. Nat. Med. *15*, 946–950.

Siffrin, V., Radbruch, H., Glumm, R., Niesner, R., Paterka, M., Herz, J., Leuenberger, T., Lehmann, S.M., Luenstedt, S., Rinnenthal, J.L., et al. (2010). In vivo imaging of partially reversible th17 cell-induced neuronal dysfunction in the course of encephalomyelitis. Immunity *33*, 424–436.

Smolders, J., Heutinck, K.M., Fransen, N.L., Remmerswaal, E.B.M., Hombrink, P., Ten Berge, I.J.M., van Lier, R.A.W., Huitinga, I., and Hamann, J. (2018). Tissue-resident memory T cells populate the human brain. Nat. Commun. *9*, 4593.

Sommer, A., Marxreiter, F., Krach, F., Fadler, T., Grosch, J., Maroni, M., Graef, D., Eberhardt, E., Riemenschneider, M.J., Yeo, G.W., et al. (2018). Th17 lymphocytes induce neuronal cell death in a human iPSC-based model of Parkinson's disease. Cell Stem Cell *23*, 123–131.e6.

Stellwagen, D., and Malenka, R.C. (2006). Synaptic scaling mediated by glial TNF-α. Nature *440*, 1054–1059.

Sutton, C.E., Lalor, S.J., Sweeney, C.M., Brereton, C.F., Lavelle, E.C., and Mills, K.H.G. (2009). Interleukin-1 and IL-23 induce innate IL-17 production from gammadelta T cells, amplifying Th17 responses and autoimmunity. Immunity *31*, 331–341.

Tapia-Arancibia, L., Aliaga, E., Silhol, M., and Arancibia, S. (2008). New insights into brain BDNF function in normal aging and Alzheimer disease. Brain Res. Brain Res. Rev. *59*, 201–220.

Waisman, A., Hauptmann, J., and Regen, T. (2015). The role of IL-17 in CNS diseases. Acta Neuropathol. *129*, 625–637.

Yang, S.H., Kim, J., Lee, M.J., and Kim, Y. (2015). Abnormalities of plasma cytokines and spleen in senile APP/PS1/Tau transgenic mouse model. Sci. Rep. *5*, 15703.

Yang, J., Kou, J., Lalonde, R., and Fukuchi, K.I. (2017). Intracranial IL-17A overexpression decreases cerebral amyloid angiopathy by upregulation of ABCA1 in an animal model of Alzheimer's disease. Brain Behav. Immun. *65*, 262–273.

You, T., Bi, Y., Li, J., Zhang, M., Chen, X., Zhang, K., and Li, J. (2017). IL-17 induces reactive astrocytes and up-regulation of vascular endothelial growth factor (VEGF) through JAK/STAT signaling. Sci. Rep. *7*, 41779.

Zenaro, E., Pietronigro, E., Della Bianca, V., Piacentino, G., Marongiu, L., Budui, S., Turano, E., Rossi, B., Angiari, S., Dusi, S., et al. (2015). Neutrophils promote Alzheimer's disease-like pathology and cognitive decline via LFA-1 integrin. Nat. Med. *21*, 880–886.

Zhang, J., Ke, K.-F., Liu, Z., Qiu, Y.-H., and Peng, Y.-P. (2013). Th17 cell-mediated neuroinflammation is involved in neurodegeneration of Aβ1-42-induced Alzheimer's disease model rats. PLoS ONE *8*, e75786.

Zimmermann, J., Krauthausen, M., Hofer, M.J., Heneka, M.T., Campbell, I.L., and Müller, M. (2013). CNS-targeted production of IL-17A induces glial activation, microvascular pathology and enhances the neuroinflammatory response to systemic endotoxemia. PLoS ONE *8*, e57307.

Brosseron F, Krauthausen M, Kummer M, Heneka MT. Body fluid cytokine levels in mild cognitive impairment and Alzheimer's disease: a comparative overview. Mol Neurobiol. 2014 Oct;50(2):534-44. doi: 10.1007/s12035-014-8657-1. Epub 2014 Feb 25. PMID: 24567119; PMCID: PMC4182618.

STAR★METHODS

KEY RESOURCES TABLE

REAGENT or RESOURCE	SOURCE	IDENTIFIER
Antibodies		
Brilliant Violet 510 anti-mouse CD45 (Clone 30-F11),	Biolegend	Cat# 103138, RRID AB_2563061
FITC anti-mouse CD45 (Clone 30-F11),	Biolegend	Cat# 103107, RRID AB_312972
Brilliant Violet 711 anti-mouse CD3 (Clone 145-2C11),	Biolegend	Cat# 100349, RRID AB_2565841
APC anti-mouse TCRd (Clone GL3),	Invitrogen	Cat# 17-5711-82, RRID AB_842756
eFluor450 anti-mouse TCRd (Clone GL3),	Invitrogen	Cat# 48-5711-82, RRID AB_2574071
Brilliant Violet 605 anti-mouse CD4 (Clone GK1.5)	Biolegend	Cat# 100451, RRID AB_2564591
PerCP/Cyanine5.5 anti-mouse CD8a (Clone 53-6.7)	Biolegend	Cat# 100734, RRID AB_2075238
PE/Cyanine7 anti-mouse NK1.1 (Clone S17016D)	Biolegend	Cat# 156514, RRID AB_2888852
Brilliant Violet 421 anti-mouse CCR6 (Clone 29-2L17)	Biolegend	Cat# 129818, RRID AB_11219003
PE/Cyanine7 anti-mouse F4/80 (Clone BM8),	Biolegend	Cat# 12311, RRID AB_893478
Brilliant Violet 605 anti-mouse CD44 (Clone IM7)	Biolegend	Cat# 103047, RRID AB_2562451
PE anti-mouse CD69 (Clone H1.2F3)	Biolegend	Cat# 104508, RRID AB_313111
Brilliant Violet 711 anti-mouse CD11b (Clone M1/70)	Biolegend	Cat# 101242, RRID AB_2563310
FITC anti-mouse CD62L (Clone MEL-14)	Biolegend	Cat# 104406, RRID AB_313093
PE/Cyanine7 anti-mouse TCRVg4 (Clone UC3-10A6),	Biolegend	Cat# 137707, RRID AB_10899574
APC anti-mouse TCRVg1 (Clone 2.11),	Biolegend	Cat# 141107, RRID AB_10897806
Brilliant Violet 711 anti-mouse Ly6G (Clone 1A8)	Biolegend	Cat# 127643, RRID AB_2565971
PerCP/Cyanine5.5 anti-mouse Ly6C (Clone HK1.4)	Biolegend	Cat# 128012, RRID AB_1659241
APC anti-mouse IL-1R (Clone JAMA-147)	Biolegend	Cat# 113509, RRID AB_2264757
PE anti-mouse/human Ki-67 (Clone 11F6),	Biolegend	Cat# 151210, RRID AB_2716008
FITC anti-mouse IL-17A (Clone TC11-18H10.1)	Biolegend	Cat# 506908, RRID AB_536010
PE anti-mouse IFN-g (Clone XMG1.2),	Biolegend	Cat# 505808, AB_315402
Brilliant Violet 421 anti-mouse TNF-a (Clone MP6-XT22)	Biolegend	Cat# 506328, RRID AB_2562902
APC anti-mouse RORgt (Clone AFKJS-9)	Invitrogen	Cat# 17-6988-82, RRID AB_10609207
PE/Cyanine7 anti-mouse Tbet (Clone 4B10),	Invitrogen	Cat# 25-5825-82, RRID AB_11042699
inVivoMAb anti-mouse IL-17A (Clone 17F3)	BioXCell	Cat #BE0173, RRID: AB_10950102
InVivoMAb mouse IgG1 isotype control (MOPC-21)	BioXCell	Cat #BE0083, RRID: AB_1107784
anti-Aβ (6E10)	Covance	Cat #SIG-39340, RRID AB_2564652
anti-APP (C17)	This paper	N/A
anti- C-terminal fragments (CTF)	This paper	N/A
anti-Tau N-Ter (M19G)	This paper	N/A
anti-Tau C-ter	This paper	N/A
anti-tau phosphorylation at S199	This paper	N/A
anti-phospho-Tau (Ser202, Thr205) (AT8)	Millipore	Cat # MN1020, RRID: AB_223647
anti-phospho-Tau (Ser396) Polyclonal Antibody	ThermoFisher Scientific	Cat #44-752G, RRID: AB_2533745
anti-phospho-Tau (Ser262) Polyclonal Antibody	ThermoFisher Scientific	Cat#44-750G, RRID: AB_2533743
anti-phospho-Tau (Ser404) Polyclonal Antibody	ThermoFisher Scientific	Cat#44-758G, RRID: AB_2533746
anti-phospho-Tau (Thr212, Ser214) (AT100)	ThermoFisher Scientific	Cat# MN1060, RRID: AB_223652
anti-Tau-1 (PC1C6)	Millipore	Cat #MAB3420, RRID: AB_94855
Peroxidase labeled goat anti-rabbit	Vector Laboratories	PI-1000
Peroxidase labeled horse anti-mouse	Vector Laboratories	PI-2000
Iba1 polyclonal Antibody	Wako	019-197441
GFAP polyclonal Antibody	Dako	Z0334

(*Continued on next page*)

Continued

REAGENT or RESOURCE	SOURCE	IDENTIFIER
Chemicals, peptides, and recombinant proteins		
Complete EDTA free protease inhibitor cocktail	Merck Life Sciences	Cat#11873580001
Mouse IL-17A Recombinant Protein,	Invitrogen	Cat #34-8171-82,
Evans Blue	Sigma	E2129, CAS 314-13-6
Cresyl violet acetate	Sigma	C5042, CAS 10510-54-0.
Critical commercial assays		
LIVE/DEAD Fixable Near-IR Dead Cell Stain Kit	ThermoFisher	Cat #L10119
DC protein assay reagent kit,	Biorad	Cat#5000116
DAB (used for Aβ IHC)	Sigma	D9015
ABC kit (for Aβ IHC)	Vector Laboratories	PK6100
Amyloid beta 40 Human ELISA Kit	ThermoFisher Scientific	Cat # KHB3481
Amyloid beta 42 Human ELISA Kit	ThermoFisher Scientific	Cat # KHB3441
4%–12% NuPage Novex gels	Invitrogen	Cat # NP0323BOX
chemiluminescence kits ECL™	Amersham Bioscience	RPN2106
Experimental models: organisms/strains		
3xTg-AD C7BL/6-129SvJ mice	The Jackson Laboratory	Stock No: 34830-JAX,
WT C7BL/6-129SvJ mice	The Jackson Laboratory	Stock No: 101045,
Software and algorithms		
SMART video-tracking	Panlab	RRID SCR_002852
FlowJo	Tree Star	RRID SCR_008520
GraphPad Prism 8.0	GraphPad	RRID SCR_002798
ImageJ software	Scion Software	RRID:SCR_003070

RESOURCE AVAILABILITY

Lead contact

Further information and requests for resources and reagents should be directed to and will be fulfilled by the Lead Contact Julie C. Ribot (jribot@medicina.ulisboa.pt).

Materials availability

There are restrictions to the availability of home-made antibodies due to our need to maintain the stock. We are glad to share reagents with compensation by requestor for its processing and shipping.

Data and code availability

- All data reported in this paper will be shared by the lead contact upon request.
  - This study did not generate any code.
  - Any additional information required to reanalyze the data reported in this paper is available from the lead contact upon request.

EXPERIMENTAL MODEL AND SUBJECT DETAILS

Ethics statement

All handling, surgical, and post-operative care procedures were approved by Instituto de Medicina Molecular Internal Committee (ORBEA) and the Portuguese Animal Ethics Committee (DGAV), in accordance with the European Community guidelines (Directive 2010/63/EU) and the Portuguese law on animal care (DL 113/2013). All efforts were made to minimize the number of animals used in the study.

Mice

C7BL/6-129SvJ mice bearing three mutations (3xTg-AD) associated with familial AD (amyloid precursor protein [APPswe], presenilin-1 [PSEN1] and microtubule-associated protein tau [MAPT]) were purchased from the Mutant Mouse Research and Resource Center at The Jackson Laboratory. Mice were bred and housed at the Instituto de Medicina Molecular animal facility under conventional conditions. Male and female animals were tested at an early stage (2-3 months old (mo), i.e., when no cognitive deficits are observed),

at the onset of disease (5-6 mo, when the cognitive deficits initiate), and at later stages (8-9 mo, when pathology and memory deficits are well established) (Oddo et al., 2003a; Billings et al., 2005, 2007; Giménez-Llort et al., 2007). WT mice from the C7BL/6-129SvJ background were used as controls.

METHOD DETAILS

Behavioral Tests

Cognitive performance, as well as locomotion and anxious behavior were evaluated according to Ribeiro et al. (2019). Mice were handled for 5 days before behavioral tests, which were performed in the following sequence: open-field (OF), elevated plus maze (EPM), Y-Maze and Morris water maze (MWM). Mazes were cleaned with a 30% ethanol solution between each trial. Animals were randomized for the behavioral testing. All behavioral tests were performed during the light phase between 8 a.m. and 6 p.m, under dim light, in a sound attenuated room. Mice movements were recorded and analyzed using the video-tracking software – SMART®.

OF

The mice were placed in the center of a square apparatus, surrounded by vertical walls (66 cm × 66 cm × 66 cm) – open-field arena. They freely explored the maze for 5 min. The total distance traveled was determined. At the end of the 5 min test, mice were removed from the open-field arena and placed into its home cage.

EPM

The maze is shaped like a plus sign and consists of two ''open'' (no walls, 5 cm × 29 cm) and two ''closed'' 122 (5 cm × 29 cm × 15 cm) arms, arranged perpendicularly, and elevated 50 cm above the floor. Each animal was placed on the center of the equipment, facing an open arm, and given 5 minutes to explore the maze. The total number of transitions between the open arms and the total arms were used as anxiety and locomotor parameters as previously done in our Institute (Coelho et al., 2014).

Y-Maze

The Y-maze is a two-trial recognition test. Mice are placed in a Y-shaped maze with 3 arms (each with 35 cm length x 10 cm width x 20 cm height), angled at 120°; on the first trial (learning trial), the animal explored the maze for 10 min with only two arms opened (start and other arm); after returning to his home cage for 1 h, the same animal was re-exposed to the maze for 5 min (test trial) with the novel arm available. The time spent exploring each arm was quantified. Discrimination ratio is calculated dividing time in the N or O arm, by the sum of the time in both arms (N+O).

MWM

MWM was performed as described (Ribeiro et al., 2019) during five consecutive days and consisted of a four day acquisition phase and a one day probe test. During the acquisition phase each mouse was given four swimming trials per day (30-min intertrial interval). A trial consisted of allowing the mouse to explore and reach for the hidden platform. If the animal reached the platform before 60 s, it was allowed to remain there for 10 s; if the animal failed to find the target before 60 s, it was manually guided to the platform, where it was allowed to remain for 20 s. On the probe test, the platform was removed and animals were allowed to swim freely for 60 s while recording the percentage of time spent on each quadrant.

Surgical procedures

The ALZET Brain Infusion Kit is used for the prolonged administration of the antibody against IL-17 (1.36 mg/animal, during 6 weeks at a constant rate of 0.15 μl/hr), or mouse IgG1 as control. This dose has been determined based on previous studies (Ribeiro et al., 2019; Brosseron et al., 2014). Mice were anesthetized under 1.5% isoflurane in 100% oxygen in a transparent acrylic chamber. After induction, mice were moved to a stereotaxic frame, maintaining isoflurane anesthesia. A small incision was made in the skin between the scapulae, and a pocket was formed by spreading the connective tissues apart, for the subcutaneous placement of the mini-osmotic pump. The cannula was inserted in the right ventricle, in the following stereotaxic coordinates: 0.5 mm anterior-posterior, 1 mm medial-lateral and 2.5 mm dorsal-ventral to Bregma. The skin incision was closed with sutures. Behavior tests were performed 6 weeks after implanting the cannulas, when treatment is concluded and the mice fully recovered from surgery. For the prolonged treatment, the mini-osmotic pump was removed after the initial 6 weeks of treatment, and replaced with a new pump, filled with either aIL-17 or mouse IgG1, to prolong the treatment for another 6 weeks. Behavior was tested immediately after the conclusion of this extended treatment period. Alternatively, C57BL/6 WT mice were administered with IL-17 (0.1 mg/ml, total volume of 3 ul) or control saline solution (PBS, total volume of 3 ul) as previously described (Ribeiro et al., 2019). Briefly, mice were anesthetized under 1.5% isoflurane in 100% oxygen. A single intracerebroventricular injection was performed into the right ventricle of the brain using the stereotaxic coordinates of 0.6 mm posterior, 1.2 mm lateral, and 2.2 mm ventral to bregma. A 10 μL Hamilton syringe was used for intracerebroventricular injection. Behavioral assessment was performed 24 hours after surgery in the Y-maze.

Flow cytometry

Flow cytometry was performed according to Ribeiro et al. (2019). Mice were sacrificed with CO_2 and immediately transcardiacally perfused with ice-cold PBS. Meninges were collected and processed as previously described (Derecki et al., 2010). Brains were cut into 2 mm^2 pieces and incubated for 30 minutes at 37°C with stirring in RPMI 5% fetal bovine serum (FBS) medium supplemented with collagenase D (1.5 mg/ml; Roche) and DNase I (100 μg/mL, Roche). Supernatants were collected and live cells were isolated on a gradient of Percoll 70% - 30% (GE Healthcare). Spleens and cLNs were homogenized and washed in RPMI medium 10% FBS. Meninges and cLNs were pooled from up to 3 mice, brains and spleens were analyzed individually.

FACS stainings were performed as previously described (Ribeiro et al., 2019) using indicated monoclonal antibodies (mAbs). Dead cells were excluded using LiveDead Fixable Viability Dye (Invitrogen). Samples were acquired using FACSFortessa (BD Biosciences). Data were analyzed using FlowJo software (Tree Star).

Immunohistochemistry

For immunohistochemical studies, females were deeply anaesthetized with pentobarbital sodium (50 mg/kg, intraperitoneally), then transcardially perfused with cold NaCl (0.9%) and with 4% paraformaldehyde in PBS (pH 7.4). Brains were removed, post-fixed for 24 h in 4% paraformaldehyde and cryoprotected in 30% sucrose before being frozen at −40°C in isopentane (methyl-butane) and stored at −80°C. Coronal brains sections (35 μm) were obtained using a Leica cryostat. Free-floating sections were chosen according to the stereological rules, with the first section taken at random and every 12 sections afterward, and were stored in PBS-azide (0.2%) at 4°C.

For Aβ immunohistochemistry (IHC), sections were pretreated with 80% formic acid for 3 min and were permeabilized with 0.2% Triton X-100/sodium phosphate buffer. Sections were then blocked with 10% "Mouse On Mouse" Kit serum (Vector Laboratories) for 1 h before incubation with mouse biotinylated anti-Aβ antibody (6E10) at 4°C overnight. After washing in PBS, the sections were incubated with the ABC kit (Vector Laboratories) for 2 h and developed using DAB (Sigma). Images were acquired using Leica ICC50 HD microscope. Quantification of the 6E10 staining intensity was performed using Mercator software (Explora Nova, Mountain View, CA, USA). The number of plaques, the average plaque size and the plaque burden, expressed as percentage of analyzed area, were calculated in the cortex and hippocampus of the 3xTg-AD mice.

Evans Blue Quantification

3xTg-AD and C7BL/6-129SvJ WT mice, previously treated with either aIL-17 or IgG1, were injected *i.v.* with 1% Evans Blue dye (Sigma), and perfused with PBS 45-60 min after injection. The brain was then removed, weighted, and incubated at 37°C for 48h in N,N-dimethyl formamide. A standard curve is prepared by serially diluting the Evans Blue dye from 50 to 2,5 μg/ml. The content of dye was determined by spectrophotometer at 620 nm, subtracting absorbance at 740 nm. Evans Blue concentration was normalized to brain weight.

ELISA Measurements

Brain levels of human Aβ1-40 and Aβ1-42 were measured using ELISA kits (Invitrogen, Carlsbad, CA, USA; IBL-International, Hamburg, Germany) following manufactured' instructions. Briefly, for hippocampal and cortical samples, 20 μg of protein were diluted in Guanidine/Tris buffer (Guanidine HCl 5 M and Tris 50 mM pH 8), sonicated and incubated for 1h at 4°C under agitation. Samples were then diluted in a BSAT-DPBS solution (KCl, KH_2PO_4, NaCl, Na_2HPO_4, BSA 5%, Tween-20 0.03% pH 7.4). The homogenates were centrifuged at 12,000 g for 15 min at 4°C. Supernatants were collected for the analysis of $A\beta_{1\text{-}40}$ and $A\beta_{1\text{-}42}$ by colorimetric immunoassays. Absorbance was measured in a TECAN Infinite 200 plate reader. The amounts of Aβ were expressed as pg/mg of total protein.

Western Blots

For all biochemical experiments, tissue was homogenized in 200 μL Tris buffer (pH 7.4) containing 10% sucrose and protease inhibitors (Complete; Roche Diagnostics GmbH), sonicated, and kept at −80°C until use. Protein amounts were evaluated using the BCA assay (Pierce), subsequently diluted with LDS 2X supplemented with reducing agents (Invitrogen) and then separated on 4%–12% NuPage Novex gels (Invitrogen). Proteins were transferred to nitrocellulose membranes, saturated (5% non-fat dry milk or 5% BSA) in TNT (Tris 15 mM pH 8, NaCl 140 mM, 0.05% Tween) and incubated with primary (APP and C-terminal fragments (CTF), home-made, 1:5000), tau (tau-1 Millipore #MAB3420, 1:10000, N-Ter, C-ter, home-made, 1:10000) and tau phosphorylation at S396 (Invitrogen #44-752G, 1:10000), S199 (home-made, 1:2000), S262 (Invitrogen #44-750G, 1:1000), S404 (Invitrogen #44-758G, 1:10000) and S212/T214 (AT100, Invitrogen #MN1060, 1:1000) overnight and then corresponding secondary antibodies (peroxidase labeled horse anti-rabbit 1/5000 or anti-mouse 1/50,000, Vector Laboratories). Immunoreactivity was visualized using chemiluminescence kits (ECL™, Amersham Bioscience) and a LAS3000 imaging system (Fujifilm). Results were normalized to GAPDH (Sigma-Aldrich) and quantifications were performed using ImageJ software (Scion Software).

Electrophysiological fEPSPs recordings

Electrophysiological fEPSP recordings were performed according to Ribeiro et al. (2019), as described in the previous section. Briefly, 3xTg-AD females and WT controls were sacrificed by cervical dislocation, the brain was rapidly removed and the hippocampi

dissected free in ice-cold Krebs solution (124 mM NaCl; 3 mM KCl; 1.25mM NaH_2PO_4; 26 mM $NaHCO_3$; 1 mM $MgSO_4$; 2 mM $CaCl_2$ and 10 mM D-glucose), previously gassed with 95% O_2 and 5% CO_2, pH 7.4. 400 μM transverse hippocampal slices were obtained with a McIlwain tissue chopper and field excitatory postsynaptic potentials (fEPSPs) were recorded in stratum radiatum of the CA1 area as previously described (Ribeiro et al., 2019). After obtaining a stable 10 minutes baseline, Input/Output (I/O) curves and long-term potentiation (LTP, 10c trains with 4 pulses at 100 Hz separated by 200 ms, induced at 0.5mV/ms) were recorded. Recordings were performed at 32°C, 3 mL/min. For the titration experiments, hippocampal slices were pre-incubated with IL17 (10ng/mL or 30ng/mL; Ebioscience) for 1 hour before LTP induction.

QUANTIFICATION AND STATISTICAL ANALYSIS

Data were analyzed using GraphPad Prism 8.0 (GraphPad, San Diego, CA). The values presented are mean ± SEM of n independent experiments. To test the significance of the differences between 2 conditions, a Student's t test, Mann-whitney and F-Test were used. In statistical tests between 3 or more conditions, a one-way ANOVA or Kurskal-Wallis Test followed by a Bonferroni's or Dunnett's multiple comparison post hoc test as specified in the figure legends. *P*-values of < 0.05 were considered to be statistically significant. Sample sizes and p values can be found in figure legends.